NANO LETTERS

2001
Vol. 1, No. 11
651−655

Environmentally-Responsive, Entirely Hydrophilic, Shell Cross-linked (SCK) Nanoparticles

Qinggao Ma, Edward E. Remsen, Tomasz Kowalewski,† Jacob Schaefer, and Karen L. Wooley*

Department of Chemistry, Washington University, One Brookings Drive, CB 1134, St. Louis, Missouri 63130-4899

Received August 17, 2001

Ⓦ **This paper contains enhanced objects available on the Internet at http://pubs.acs.org/nano.**

ABSTRACT

Precise tuning of the chemical composition of shell cross-linked (SCK) nanoparticles provides systematic control over their environmental interactions, as is demonstrated by regioselective modification of the internal and external chemistries. Hydrolysis of the poly(methyl acrylate) core domain of SCKs composed of poly(acrylic acid-*co*-acrylamide) shell layers produced entirely hydrophilic, pH responsive nanocage-like structures presenting poly(acrylic acid) chains from the inner cage surface. Two-dimensional, colloidally crystallized nanoarrays of the SCKs and nanocages when sorbed at solid substrate surfaces in the presence of water were substrate dependent and pH tunable.

Environmentally responsive polymers hold great promise as novel materials for medical and biotechnological applications.[1] Their fabrication into well-defined, robust nanomaterials provides a potential route for improved control of key performance properties such as biocompatibility,[2] targeted delivery,[3] and controlled release,[4] which could potentially extend the utility of these materials. An interesting example was recently reported by Sauer and Meier,[5] in which pH-responsive nanocapsules were prepared by templated polymerization in the lipid bilayer of unilamellar vesicles. The resulting nanocapsules, composed of cross-linked poly(acrylic acid), exhibited hydrodynamic diameters ranging from ca. 100 nm to 1000 nm, depending upon the pH and salt concentrations. Increasing pH and decreasing salt concentration gave swelling of the hollow spheres. Our interest lies in the ability to prepare environmentally responsive nanostructured materials of sub-100 nm dimensions. Our methodology employs a templating strategy that begins from the supramolecular assembly of amphiphilic block copolymers into polymer micelles, followed by their covalent stabilization through shell cross-linking, and finally manipulation of the core hydrophilicity.

The supramolecular assembly of amphiphilic block copolymers serves as a versatile synthetic strategy for preparing nanomaterials,[6] and one capable of molding environmentally responsive polymers into well-defined nanostructures. Previous studies[7] have demonstrated that cross-linking of the chain segments that constitute the shell layer covalently stabilizes polymer micelles against disruptive solution conditions and results in shell cross-linked (SCK) nanoparticles with a core−shell morphology. Subsequent chemical functionalization of the SCK can produce environmentally responsive nanoparticles. For example, SCKs containing cores of polyisoprene[8] or poly(ϵ-caprolactone)[9] can be core-degraded to yield nanocages that expand in solution and flatten when dried on a substrate. Incorporation of functional groups of different pK_a into SCKs results in hydrophilic, zwitterionic nanoparticles[10] and temperature-dependent properties,[11] as described by Armes and co-workers. In the present study, we report the synthesis and characterization of an entirely hydrophilic nanocage-like structure having a cross-linked shell of poly(acrylic acid-*co*-acrylamide) and presenting poly(acrylic acid) linear chains topologically from the inner nanocage surface.[12] The limited extent of reversible, pH-controlled swelling/deswelling for the precursor amphiphilic SCKs, relative to their entirely hydrophilic derivatives, demonstrates the fine-tuning that is possible for these systems through convenient chemical modifications within the regions of the complex morphology.

Shell cross-linked nanoparticles and nanocages having a common hydrogel-like surface of poly(acrylic acid-*co*-acrylamide) and hydrophobic poly(methyl acrylate) and hydrophilic poly(acrylic acid) core chains, respectively, were employed in these studies to evaluate the extent of reversible

† Current address: Carnegie Mellon University, Department of Chemistry, 4400 Fifth Avenue, Pittsburgh, PA 15213.

10.1021/nl0156078 CCC: $20.00
Published on Web 08/29/2001

Scheme 1

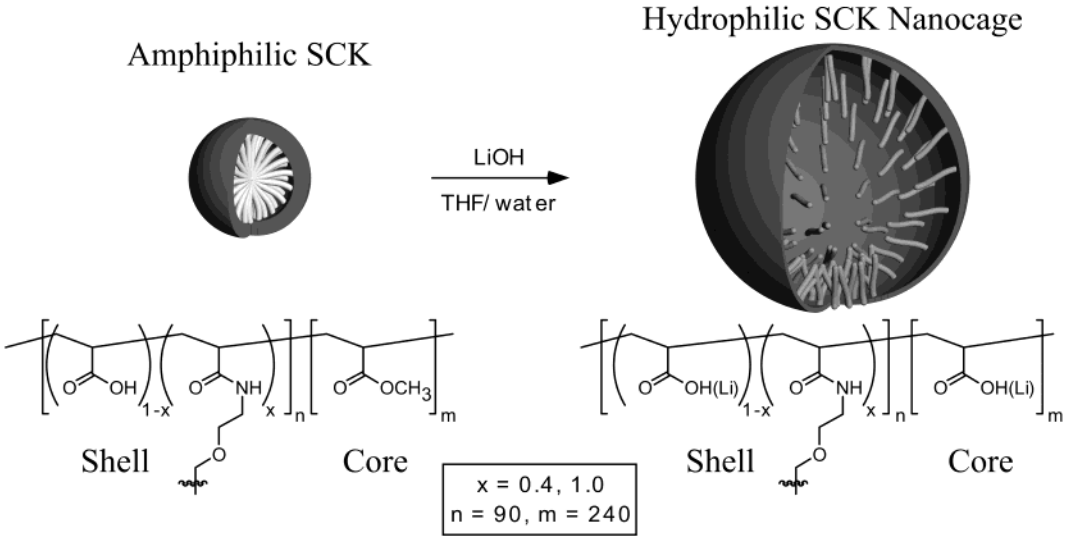

Table 1: Data for SCKs (PMA core) and Nanocages (PAA core)

				pH = 5.0		pH = 8.0	
% cross-linker	core	TEM D_{av} (nm)[a]	AFM H_{av} (nm)[b]	D_h (DLS) (nm)	zeta potential (mV)	D_h (DLS) (nm)	zeta potential (mV)
40%	PMA	30.5 ± 2.6	6.2 ± 2.2	40 ± 1	−6.2 ± 2.4	42 ± 1	−24.4 ± 6.6
40%	PAA	31.8 ± 2.6	4.3 ± 1.2	89 ± 15	−2.1 ± 1.4	108 ± 1	−24.9 ± 10
100%	PMA	34.2 ± 4.7	8.6 ± 1.6	59 ± 19	−1.5 ± 0.9	70 ± 10	−10.8 ± 7.3
100%	PAA	35.0 ± 4.5	9.8 ± 2.5	66 ± 9	−0.1 ± 0.1	92 ± 6	−2.3 ± 2.8

[a] 50 particles measured. [b] AFM height histograms are available in the Supporting Information.

pH-controlled swelling for these nanostructures with and without hydrophobic core constraints. SCKs prepared from poly(acrylic acid)-*b*-poly(methyl acrylate) (PAA_{90}-*b*-PMA_{240}) and cross-linked with 2,2′-(ethylenedioxy)bis(ethylamine) were synthesized as described previously.[13] The extent of cross-linking was controlled by the stoichiometric equivalence of amine to carboxylic acid. To evaluate the effects of the cross-linking density of the shell upon the properties of the SCKs and nanocages, SCKs with 40% and 100% nominal cross-linking were prepared.[14] Lyophilized SCKs were resuspended in THF/water (3:1), and LiOH was added to cleave selectively the methyl esters[15] in the core domain, while leaving the amide based cross-links intact (Scheme 1). Exhaustive dialysis[16] removed the hydrolysis reaction product, methanol, to yield the entirely hydrophilic nanocage. Shell cross-linking is essential for the formation of this nanostructure; the polymer micelles (D_h: 55 ± 1 nm in water by dynamic light scattering (DLS)) maintained by hydrophobic interactions among the PMA segments within the core domain disintegrated upon hydrolysis to yield PAA homopolymer (<6 nm by DLS).

Solution-state ^{1}H NMR spectroscopy confirmed the hydrolysis of the PMA within the SCK core by monitoring the disappearance of the methyl proton resonance at 3.62 ppm (300 MHz, $CDCl_3$/CD_3OD/THF-d_8 3:1:1). Solid-state ^{13}C NMR (125 MHz, magic angle spinning at 6.25 kHz) also indicated the formation of the entirely hydrophilic nanocages,[17] as determined by the disappearance of the methyl ester signal at 50 ppm and the growth of the carboxylic acid resonance at 180 ppm. The constant relative intensity observed for the cross-linker methylene signal at 68 ppm and also for the amide carbonyl carbon at 172 ppm indicated that the shell remained intact.

Conversion of the SCK core from hydrophobic to hydrophilic character provides different environments for capture and retention of guest molecules. The SCKs with hydrophobic PMA cores sequestered hydrophobic molecules, for example, iodine and chloroform. After the core hydrolysis procedure, the entirely hydrophilic nanocage structure filled with water, causing a volume increase, as observed by DLS.

The intramolecular electrostatic repulsive interactions among the ionized acrylic acid ($pK_a \sim 4.2$) repeat units cause the SCKs and nanocages to respond to pH, as observed by DLS, and this is further supported by zeta-potential measurements (Table 1).

Upon hydrolysis of the PMA core, the nanostructures underwent significant swelling. Those having a lower degree of shell cross-linking exhibited more than a 2-fold increase in hydrodynamic diameters, D_h (10- to 20-fold increase in volume), whereas a modest increase in the D_h was observed for the more highly cross-linked, entirely hydrophilic nanoparticles. At pH 8.0, well above the pK_a of the acrylic acid repeat units, the nanocages underwent more extensive swelling than was observed for the SCKs having structural restrictions imposed by the PMA core. Increasingly negative zeta-potential values at high pH suggest pH-induced deprotonation of higher proportions of the acrylic acid residues. Surprisingly, the zeta potential values for the nanocages were

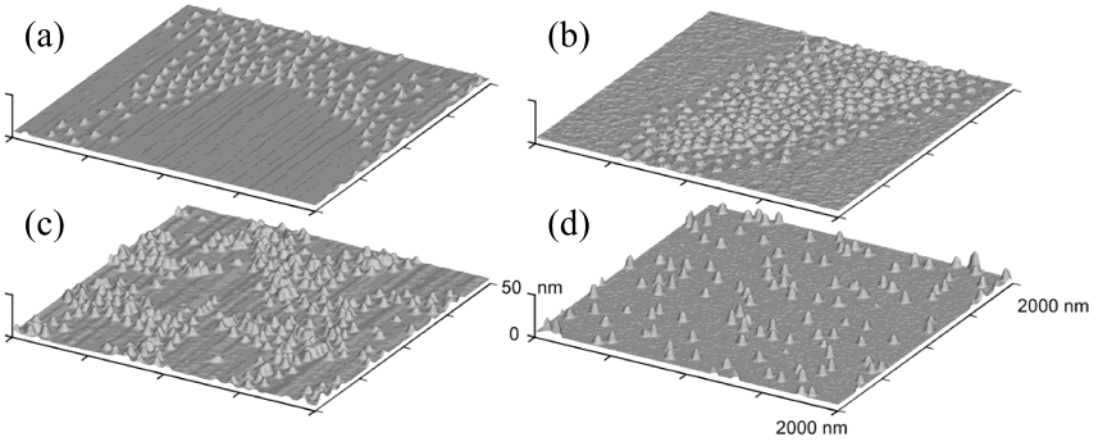

Figure 1. Tapping mode AFM height images of the nanostructures deposited from aqueous solution (0.05 mg/mL) onto freshly cleaved mica and allowed to dry freely in air. SCKs with 40% nominal degree of cross-linking: (a) PMA core; (b) PAA core. SCKs with 100% nominal degree of cross-linking: (c) PMA core; (d) PAA core.

less negative than those for the corresponding SCKs, which may be due to effects related to decreased electrophoretic mobility for the larger diameter, entirely hydrophilic nanocages. At pH values less than 5.0, significant amounts of aggregation were observed.

The diameter vs height aspect ratios for the SCKs and nanocages adsorbed onto substrates indicated substantial flattening of the nanostructures, allowed by the fluid-like PMA and solvated PAA cores, respectively. Transmission electron microscopy provided diameter determinations and atomic force microscopy (AFM) provided height measurements (Figure 1). In contrast to nanocages prepared previously by complete degradation and removal of the core material,[8,9] the remaining PAA within these new nanocages resulted in particulate materials having dimensions similar to their SCK precursors (Table 1). However, to accommodate the degree of swelling in aqueous solution, the PAA-containing nanostructures must expand into an open framework cage-like structure.

SCKs have sufficient surface charge form two-dimensional (2-D) arrays when adsorbed onto mica,[18] and this behavior was also exhibited by the nanocages. The SCKs having nominally 40% of their acrylic acid groups consumed during the shell cross-linking chemistry maintain nominally 60% of the acid functionalities, a significant portion of which can exist as carboxylates to drive electrostatic array assembly on mica. The tendency to form such regular arrays clearly decreased upon 100% nominal cross-linking (Figure 1). As shown in Figure 2a, deprotonated SCKs, having a nominal 40% conversion of the acrylic acid groups of the shell layer converted to amides, formed two-dimensional arrays on mica when $MgCl_2$ was added to the solution. The salt presumably binds the polyanionic SCK to the negatively charged mica surface through Mg^{2+} bridges. This interpretation is supported by the formation of arrays using $ZnCl_2$ in place of $MgCl_2$. The solution concentration of $MgCl_2$ controlled the kinetics of array formation, and adjustment of the salt concentration to 10 mM slowed the kinetics sufficiently for real-time monitoring of array formation by in situ fluid tapping AFM as depicted in the movie associated with Figure 2a (movie 1). Nanoarray assembly proceeded through the initial formation of islands of nanoparticles. The array assembly continued by further SCK binding to the mica substrate to fill the spaces between the islands.

In the case of hydrophobic graphite surfaces, 2-D arrays formed in the absence of salt as shown in Figure 2b and its associated movie (movie 2). During the initial stages of the 2-D colloidal array formation, the particle assembly appears to be dominated by particle−particle repulsive interactions. Once adsorbed onto the graphite substrate, it is evident that the particles retain sufficient mobility to diffuse across the substrate surface and continue to refine the 2-D crystalline structure, resembling, qualitatively, alignment along the graphite steps.

Array formation on graphite was strongly dependent also on solution pH, and dynamic changes were triggered by protonation of the nanoparticles through the addition of a concentrated solution of potassium hydrogen phthalate (KHP). Protonation disrupted the 2-D arrays on a time scale slow enough to be captured by in situ fluid tapping AFM as shown in the movie corresponding to Figure 2c (movie 3). After the introduction of KHP, the SCKs became increasingly protonated over time, which diminished the interparticle spacing (D_{IP}) within the arrays, and finally resulted in aggregation characterized by local clustering and the formation of many voids. Addition of potassium hydroxide reversed this process, leading to aggregate dissociation and 2-D array reformation as shown in the movie corresponding to Figure 2d (movie 4).

In summary, we have demonstrated that shell cross-linking of polymer micelles can allow further functionalization of the SCK core to produce entirely hydrophilic SCK nanocage structures. Importantly, the degree of shell cross-linking dictates the chemical composition and physical constraints that then control the properties of the nanocages. The thermodynamic and kinetic parameters during the substrate-induced colloidal assembly are of great interest, and these features will be explored further. The nanoengineered SCKs have complex morphologies and estimated molecular weights of several million Daltons (based on previous absolute

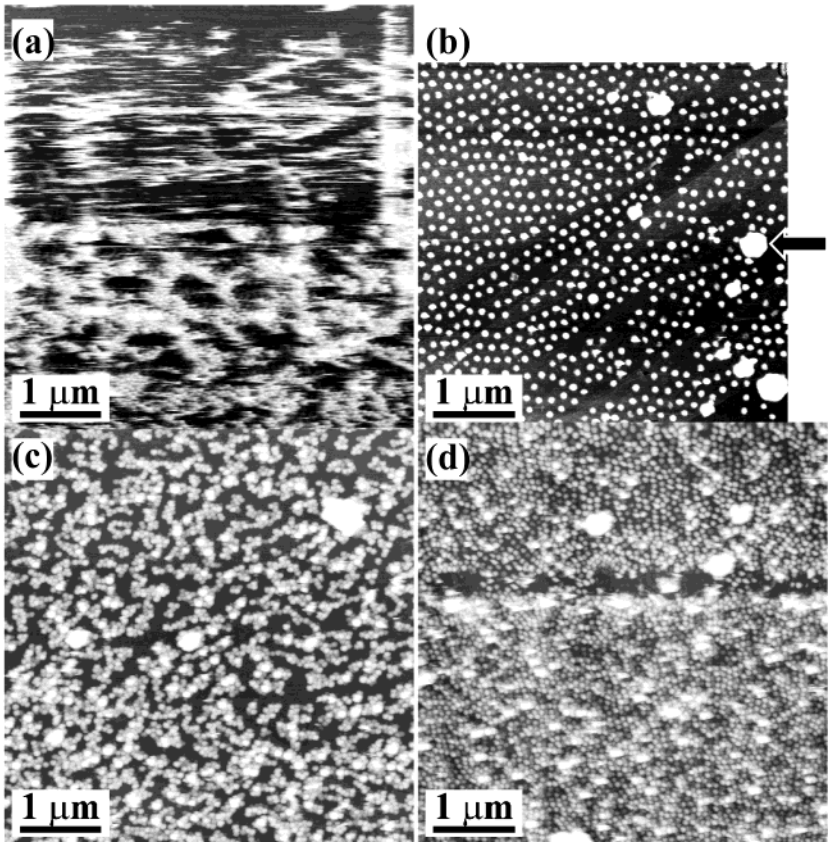

Figure 2. Still images representing movies 1, 2, 3, and 4 from fluid tapping AFM images. All SCKs shown had a nominal 40% degree of cross-linking. Scan sizes are 5 × 5 micron and 256 s per frame. (a) Still image of the first frame of movie 1. This movie shows SCK nanoparticle binding to the mica surface to form ordered 2-D arrays. AFM imaging conditions: 30 μL on mica containing 0.1 mg/mL SCK, 20 mM HEPES, pH 6.8, 10 mM $MgCl_2$. (b) Still image of the ninth frame of Movie 2. This movie demonstrates the dynamic character of 2-D SCK arrays on a hydrophobic graphite surface. AFM imaging conditions: 30 μL on graphite containing 0.1 mg/mL SCK, 20 mM HEPES, pH 6.8. The AFM image frames were aligned against the large particle indicated by the arrow, and cropped to a 4.5 × 4.5 μm area. (c) Still image of the fifteenth frame of Movie 3. This movie shows the disruption of 2-D arrays on graphite via protonation using potassium hydrogen phthalate (KHP) buffer solution. AFM imaging conditions: 30 μL on graphite containing 0.1 mg/mL SCK, 20 mM HEPES, 167 mM KHP, pH 4.5. (d) Still image of the fifteenth frame of Movie 4. This movie shows the dissociation of protonated aggregates of SCKs by the addition of base. AFM imaging conditions: 30 μL on graphite containing 0.1 mg/mL SCK, 20 mM HEPES, 167 mM KHP, pH 4.5 + 5 μL of 1 M KOH. Final solution pH was 6.5.

Ⓦ Movies Ⓦ 1, Ⓦ 2, Ⓦ 3, and Ⓦ 4 are available in Quicktime (.qt) format.

molecular weight determinations by sedimentation equilibrium for SCKs of comparable hydrodynamic diameter)[19] and are expected to be used as versatile drug delivery vehicles to prolong the residence time of drugs in contact with mucosal membranes.[20] Moreover, the high degree of control over the composition of the polymer chains comprising the SCK core domain will lead to enhanced guest loading and release profiles.[21]

Acknowledgment. The authors thank Brookhaven Instruments Co. (Holtsville, NY) for providing a ZetaPALS instrument for zeta potential measurement. The authors also thank Mr. G. Michael Veith for his acquisition of TEM images and Mr. Christopher G. Clark, Jr. for generating nanoparticle illustrations. Funding of this research by the National Science Foundation DMR-9974457 (K.L.W.) and DMR-0097202 (J.S.), and by a DURIP grant DAAG55-98-1-0046 (K.L.W.) is gratefully acknowledged.

Supporting Information Available: ^{13}C CPMAS NMR spectra, histograms of AFM height data. This material is available free of charge via the Internet at http://pubs.acs.org.

References

(1) Chen, G.; Hoffman, A. S. *Nature* **1995**, *373*, 49.
(2) Langer, R. *Acc. Chem. Res.* **2000**, *33*, 94.
(3) Liu, J.; Zhang, Q.; Remsen, E. E.; Wooley, K. L. *Biomacromolecules* **2001**, *2*, 362.
(4) Na, K.; Park, K.-H.; Kim, S. W.; Bae, Y. H. *J. Controlled Release* **2000**, *69*, 225.
(5) Sauer, M.; Meier, W. *Chem. Commun.* **2001**, 55.
(6) Zhang, L.; Eisenberg, A. *Science* **1995**, *268*, 1728.
(7) (a) Huang, H.; Kowalewski, T.; Remsen, E. E.; Gertzmann, R.; Wooley, K. L. *J. Am. Chem. Soc.* **1997**, *119*, 11653. (b) Huang, H.; Wooley, K. L.; Remsen, E. E. *Chem. Commun.* **1998**, *13*, 1415. (c) Murthy, K. S.; Ma, Q.; Clark, C. G., Jr.; Remsen, E. E.; Wooley, K. L. *Chem. Commun.* **2001**, 773. (d) Ding, J.; Liu, G. *Macromolecules* **1998**, *31*, 6554. (e) Sanji, T.; Nakatsuka, Y.; Kitayama, F.; Sakurai, H. *Chem. Commun.* **1999**, 2201. (f) Bütün, V.; Wang, X.-S.; Banez, M. V. de Paz; Robinson, K. L.; Billingham, N. C.; Armes, S. P.; Tuzar, Z. *Macromolecules* **2000**, *33*, 1. (g) Cao, L.; Manners, I.; Winnik, M. A. *Macromolecules* **2001**, *34*, 3353.

(8) Huang, H.; Remsen, E. E.; Kowalewski, T.; Wooley, K. L. *J. Am. Chem. Soc.* **1999**, *121*, 3805.
(9) Zhang, Q.; Remsen, E. E.; Wooley, K. L. *J. Am. Chem. Soc.* **2000**, *122*, 3642.
(10) Bütün, V.; Lowe, A. B.; Billingham, N. C.; Armes, S. P. *J. Am. Chem. Soc.* **1999**, *121*, 4288.
(11) Bütün, V.; Billingham, N. C.; Armes, S. P. *J. Am. Chem. Soc.* **1998**, *120*, 12135.
(12) In other SCKs, it has been found that conformational changes result when the core chains are well-solvated, leading to an inverted SCK from permeation of the chains through the shell and presentation to the external cage surface (unpublished results).
(13) Ma, Q.; Wooley, K. L. *J. Polym. Sci., Part A: Polym. Chem.* **2000**, *38*, 4805.
(14) Nominal cross-linking is the theoretical extent of cross-linking that could occur, based upon the amine-to-carboxylic acid stoichiometry. Solid-state NMR is used to determine the conversion of carboxylic acid groups to amides; however, whether those amide groups are part of an intrachain loop vs an interchain cross-link is not known. Huang, H.; Wooley, K. L.; Schaefer, J. *Macromolecules* **2001**, *34*, 547.
(15) Dayal, B.; Salen, G.; Toome, B.; Tint, G. S.; Shefer, S.; Padia, J. *Steroids* **1990**, *55*, 233.
(16) Note: the SCKs were dialyzed (molecular weight cutoff MWCO 12 000−14 000) against deionized water for 10 days.
(17) For experimental details, see: Huang, H.; Wooley, K. L.; Schaefer, J. *Macromolecules* **2001**, *34*, 547.
(18) Ma, Q.; Remsen, E. E.; Kowalewski, T.; Wooley, K. L. *J. Am. Chem. Soc.* **2001**, *123*, 4627.
(19) Remsen, E. E.; Thurmond, K. B. II; Wooley, K. L. *Macromolecules* **1999**, *32*, 3685.
(20) Patel, D.; Smith, A. W.; Grist, N.; Barnett, P.; Smart, J. D. *J. Controlled Release* **1999**, *61*, 175.
(21) Antipov, A. A.; Sukhorukov, G. B.; Donath, E.; Möhwald, H. *J. Phys. Chem. B* **2001**, *105*, 2281.

NL0156078